Large-scale magnetic field inversions at sector boundaries

N. U. Crooker
Center for Space Physics, Boston University, Boston, Massachusetts, USA

S. W. Kahler
Air Force Research Laboratory, Space Vehicles Directorate, Hanscom Air Force Base, Massachusetts, USA

D. E. Larson and R. P. Lin
Space Science Laboratory, University of California, Berkeley, California, USA

Received 8 October 2003; revised 30 November 2003; accepted 10 December 2003; published 26 March 2004.

[1] During the declining phase of the last solar cycle the Wind spacecraft observed a quasi-recurrent pattern of mismatches between sector boundaries identified in suprathermal electron pitch angle spectrograms and in magnetic field data alone. Intervals of mismatch imply the presence of magnetic fields that are locally inverted or turned back on themselves in a way that is intrinsic to the sector boundary. We analyze eight cases of inversion during nine successive solar rotations in 1994–1995. These range in duration from 15 to 53 hours. In most the inversions are incomplete in a systematic way: Rather than pointing opposite to its true polarity along the Parker spiral, the magnetic field hovers at an orientation more nearly orthogonal to it, always in the sense of decreasing azimuth angle. The inversion pattern is consistent with passage through coronal streamer belt loops, in which the polarity of the two legs of each loop matches the sector structure and where one leg has been released from the Sun through interchange reconnection. There are four possible variations of this pattern, depending on the sense of polarity change across the sector boundary and on whether the leading or trailing leg has been released. The latter determines whether the sector boundary or the local field reversal passes first. Three of the four variations are represented in the eight cases. Plasma parameters in the inversions are typical of the slow wind. While some cases display signatures of interplanetary coronal mass ejections, many do not. Thus the inversions may represent the quiet, quasi-steady end of a spectrum of large-scale transient outflows. *INDEX TERMS:* 2134 Interplanetary Physics: Interplanetary magnetic fields; 2111 Interplanetary Physics: Ejecta, driver gases, and magnetic clouds; 2169 Interplanetary Physics: Sources of the solar wind; *KEYWORDS:* heliospheric current sheet, coronal mass ejection

Citation: Crooker, N. U., S. W. Kahler, D. E. Larson, and R. P. Lin (2004), Large-scale magnetic field inversions at sector boundaries, *J. Geophys. Res.*, *109*, A03108, doi:10.1029/2003JA010278.

1. Introduction

[2] The heliosphere is divided into two volumes, or sectors, of open magnetic field lines with opposite magnetic polarity, and these are separated by a warped, heliomagnetic equatorial surface that forms the sector boundary. The sector boundary is nearly always assumed to be synonymous with the heliospheric current sheet (HCS), which effects a reversal in the local magnetic field from toward to away from the Sun (or vice versa) along the Parker spiral. With the advent of solar electron observations capable of identifying the sector boundary independent of local field orientation, however, came the discovery that this assumption does not always hold. Using electrons with energies >2 keV, *Kahler and Lin* [1994, 1995] found sector boundaries without field reversals and field reversals without sector boundaries. While the latter, which are much more numerous, are commonly treated as signatures of localized current sheets formed by field inversions independent of sector boundaries [e.g., *Kahler et al.*, 1996; *Crooker et al.*, 1996a; *Szabo et al.*, 1999], until now, the former have eluded interpretation. This paper analyzes cases of sector boundaries without field reversals, demonstrates that they are paired with field reversals without sector boundaries, and offers an interpretation in terms of transient streamer belt outflows.

0148-0227/04/2003JA010278$09.00

2. Analysis

[3] The study uses Wind data from December 1994 to August 1995, when the spacecraft was immersed in a relatively stable two-stream, four-sector flow pattern [e.g., *Crooker et al.*, 1996b]. Suprathermal ($E > \sim 80$ eV) electron data were obtained from the Three-Dimensional Plasma and

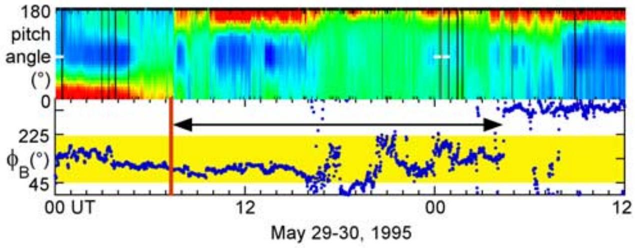

Figure 1. Wind 3DP and MFI data showing mismatched polarity reversal signatures in a 320 eV electron pitch angle spectrogram (top) and in the azimuth angle ϕ_B of the magnetic field (bottom). The double-headed arrow marks the 21 hour interval between the pitch angle shift of intense electron flux (red) from 0° to 180°, marking true passage from the away to the toward sector, and the reversal of the local field from the away (yellow) to the toward direction.

Energetic Particle Experiment (3DP) [*Lin et al.*, 1995], and solar wind ion and magnetic field data were obtained from the Solar Wind Experiment (SWE) [*Ogilvie et al.*, 1995] and the Magnetic Field Investigation (MFI) [*Lepping et al.*, 1995], respectively.

[4] Sector boundaries were identified in 320 eV electron pitch angle spectrograms [cf. *Crooker et al.*, 2004] (hereinafter referred to as Paper 1). An example is shown in the top panel of Figure 1. The red traces, first at the bottom (0°) and then at the top (180°), indicate an intense beam of electrons directed first parallel and then antiparallel to the magnetic field. Since the beam, or strahl, is always directed away from the Sun along magnetic field lines, independent of any field line contortions, the spectrogram shows an incontrovertible passage from an away sector to a toward sector at 0720 UT on 29 May 1995. While the term "sector boundary" is often used in a general way, here we limit its use to mean a true sector boundary as identified in the top panel of Figure 1.

[5] What usually serve as sector boundary signatures are changes in local magnetic field azimuth angle ϕ_B from one sector to another, where the toward and away sectors are centered on the average Parker spiral directions of 315° and 135°, respectively. Time variations of ϕ_B were scanned for these changes at or near sector boundaries. The second panel of Figure 1 gives the time variations of ϕ_B for the period matching the spectrogram. At the sector boundary, marked by the red vertical line, ϕ_B shows no change at all. It remains steadily in the away sector, shaded yellow, until 1600 UT. After that time, ϕ_B occasionally dips into the toward sector but lies predominantly in the away sector until 0420 UT on 30 May. We thus classify this case as a 21 hour mismatch between the sector boundary and the local field reversal.

[6] With brief consideration of the pattern of mismatch in Figure 1, it becomes obvious that a sector boundary without a field reversal must be paired with a field reversal without a sector boundary because eventually, the magnetic field must match the polarity given in the spectrogram. In this case, then, the field reversal without a sector boundary is not the signature of a current sheet independent of the sector boundary, as these cases usually are treated, but rather must reflect some intrinsic property of the sector boundary. This topic is addressed further in section 3.

[7] To obtain an overview of how often mismatches occur, Figure 2 shows 27 day recurrence plots of ϕ_B for nine solar rotations. Beginning on 14 December, when pitch angle spectra relatively free of contamination from bow shock-accelerated electrons became available, vertical red lines mark sector boundaries, and pink blocks mark intervals that contain sector boundaries. The exact times of the boundaries in these pink intervals cannot be determined owing to contamination by bow shock electrons or nearly isotropic electron spectra in regions of high plasma beta [*Crooker et al.*, 2003]. High beta is common at sector boundaries owing to the presence of plasma sheets, but most of these are shorter than the width of the red lines and thus are not indicated in Figure 2. (See Paper 1 for a list of the times and intervals of the sector boundaries in Figure 2 and for further information on how they were identified.) The horizontal grid lines at 45° and 225° mark the boundaries of sectors centered on the average Parker spiral directions. Black bars along the 225° grid line indicate intervals of mismatch between true sector boundaries and field reversals, i.e., magnetic field excursions from one sector to the other. While mismatch intervals as short as 25 min have been found, only those longer than 8 hours are marked since the focus of this study is on large-scale events. (Two ~5 hour mismatches on 17–18 December are illustrated in Paper 1.)

[8] From a global perspective, Figure 2 shows a relatively steady pattern of four sector boundaries per solar rotation, some of which are multiple. The pattern is occasionally broken by intrasector boundaries [*Kahler et al.*, 1996], for example, the pair on 21–22 April, with the preceding sector boundary displaced to the preceding rotation on 18 April. (Not all intrasector boundaries have been identified, as discussed in Paper 1.) Figure 2 shows many field reversals without sector boundaries, as noted by *Szabo et al.* [1999], but most of the sector boundaries align with field reversals. This is true even when all of the smaller-scale mismatches are taken into account. Of the total of 52 sector boundaries (counting multiples individually), Paper 1 categorizes 17 (33%) as lacking current sheets, implying cases of mismatch. In Figure 2 the large-scale mismatches marked with black bars occur once per solar rotation, except for the second to last. The total of eight large-scale mismatches in nine rotations with four sectors yields an occurrence rate of 22% (ignoring intrasector and multiple boundaries). Five of these eight mismatches occur in a quasi-recurrent pattern at the third of the four sector boundaries per rotation. Figure 2 shows these successively in the first three rotations, then alternately in the next four.

[9] Properties of the eight large-scale mismatch cases are listed in Table 1. The first two columns give the date and time of the sector boundary, the third column gives the date and time of the field reversal, and the fourth column gives the difference, i.e., the duration of the mismatch. With the exception of the 8 February case, with a particularly long duration of 53 hours, these range from 15 to 24 hours. The fifth column indicates the likelihood of an interplanetary coronal mass ejection (ICME) in the mismatch interval, as discussed at the end of this section, the sixth column lists the sense of polarity change across the sector boundary, from toward to away (T–A) or vice versa, and the seventh column indicates the polarity of ϕ_B. The final column,

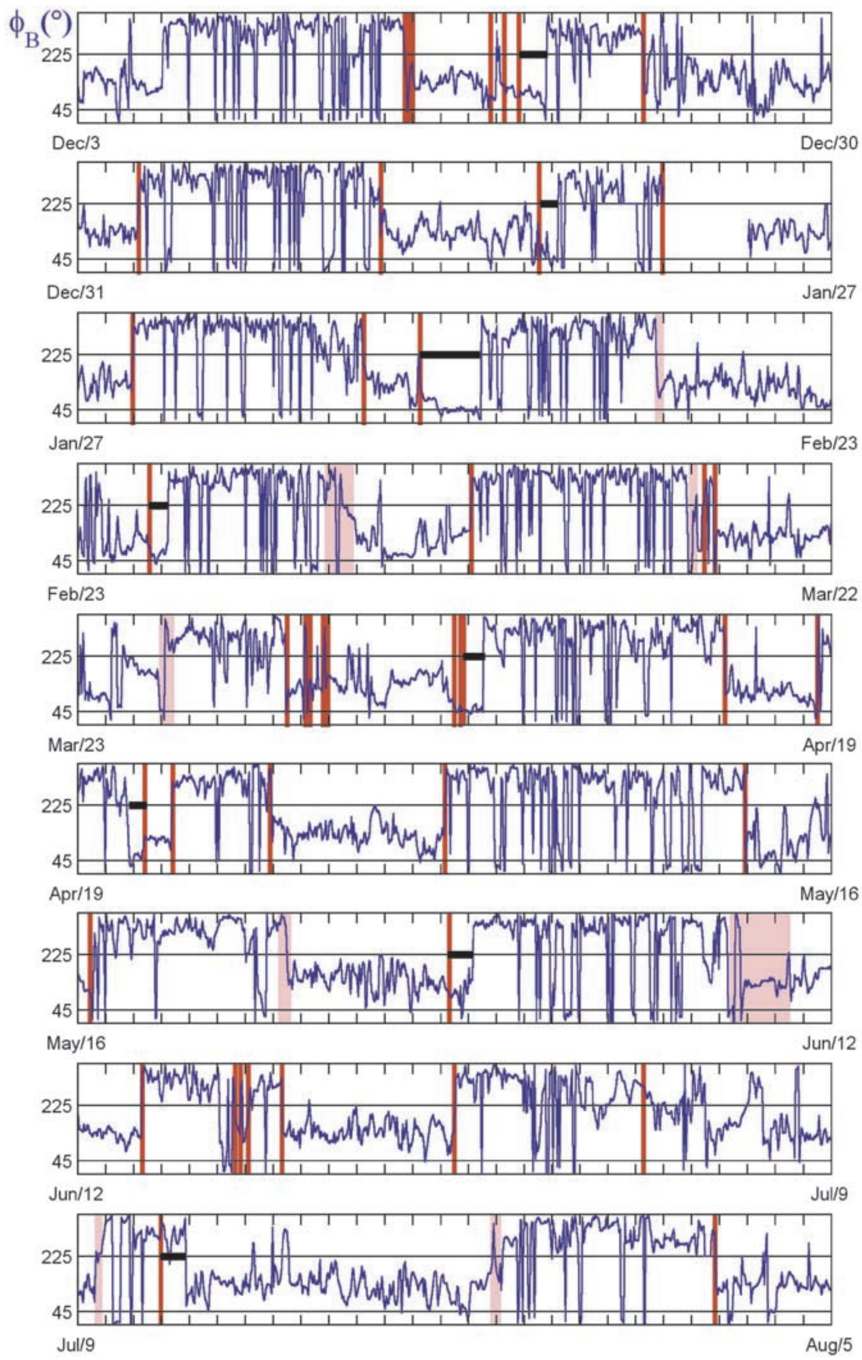

Figure 2. Twenty-seven day recurrence plots of the Wind MFI magnetic azimuth angle ϕ_B (GSE coordinates) spanning nine solar rotations from December 1994 to August 1995. Red lines (some overlapping) mark true sector boundaries identified in 3DP electron spectrograms, pink intervals contain true sector boundaries inferred from the spectrograms, and horizontal black bars mark mismatches between true sector boundaries and local polarity reversals in ϕ_B.

discussed in section 3, uses the information in the sixth and seventh columns to classify each case according to a proposed topological configuration.

[10] A close look at ϕ_B in the intervals of mismatch in Figure 2 reveals that in most cases the field does not continue to point along the Parker spiral in a sense opposite to its true polarity, as it does for many hours in Figure 1, but rather hovers at an angle nearly orthogonal to the Parker spiral. Figure 3 illustrates this effect in a scatterplot of all hourly averages of ϕ_B against the field elevation angle θ_B in the mismatch intervals. For the 11 July case, which is the only case where ϕ_B lies in the toward sector, the ϕ_B values were reduced by 180° to transform them to a virtual away sector. The plot shows a systematic displacement of the

Table 1. Mismatches Between Sector Boundaries and Magnetic Field Reversals[a]

SB Date	SB Time, UT	B Reversal Date	B Reversal Time, UT	Mismatch Duration, hours	ICME?	SB Sense	Inverted B Direction	Figure 4 Type
18 Dec. 1994	1720–1930	19 Dec.	1740	24	?	A–T	A	1
16 Jan. 1995	1220	17 Jan.	0440	16	no	A–T	A	1
8 Feb. 1995	0405–0615	10 Feb.	~1100	53	yes	A–T	A	1
25 Feb. 1995	1430	26 Feb.	0615	16	no	A–T	A	1
5 April 1995	2045	6 April	1240	16	??	A–T	A	1
21 April 1995	0820–1030	20 April	~1800	15	??	T–A	A	4
29 May 1995	0720	30 May	0420	21	no	A–T	A	1
11 July 1995	~2300	12 July	2110	22	no	T–A	T	2

[a]SB, sector boundaries; B, magnetic field; ??, contained only one ICME signature.

points to the left of the cross marking the away Parker spiral direction, toward the ortho-Parker-spiral direction of $\phi_B = 45°$. Some points extend to even smaller values of ϕ_B, into the toward sector, where they then match the true polarity, but these are in the minority. Figure 3 also shows a relatively wide spread in elevation angle θ_B. The median of the absolute value of θ_B is 27° compared to 17° for the entire Figure 2 data set. Both the systematic shift to lower ϕ_B values and the wider range of θ_B values are also present in a similar plot of all inverted fields compared to normal fields in the ISEE 3 data set [*Kahler et al.*, 1998].

[11] Plots of plasma parameters in the mismatch intervals have been analyzed for any persistent patterns, but none were found. The parameters are highly variable, as is typical in the slow wind. The 8 February case is notable for a pronounced signature of an ICME, specifically, a magnetic cloud, which covers about the first 14 hours of the 53 hour mismatch interval [*Crooker et al.*, 1998a]. Within the cloud are two short periods of counterstreaming suprathermal electrons, implying field lines attached to the Sun at both ends, another ICME signature, but most of the cloud was magnetically open. Ion temperature depressed below the value predicted from solar wind speed, a more general ICME as well as cloud signature [*Richardson and Cane*, 1995], occurred throughout the 8 February mismatch interval. Two other cases, 18 December and 5 April, displayed mildly depressed temperatures, and the 18 December case as well as the 21 April case contained short intervals of counterstreaming electrons. The remaining four cases (half) displayed no ICME signatures. The last column of Table 1 summarizes these findings by indicating the likelihood of an ICME within each mismatch interval. Cases with two question marks contained only one ICME signature.

3. Interpretation

[12] Since the true polarity of the magnetic fields in the mismatch intervals does not match the polarity of the locally measured field, the fields in the mismatch intervals must be inverted or turned back on themselves. While this is also true in intervals across which the true polarity remains the same but the local field reverses polarity, i.e., in intervals without sector boundaries, in this case the sector boundary is an intrinsic part of the signature. In mismatch intervals without sector boundaries the field reversal is interpreted in terms of a localized current sheet, whereas in the cases presented here the field reversal is the heliospheric current sheet (HCS), and it is separated from the true sector boundary. In a preliminary study of this seeming paradox, *Crooker* [2003] points out that the true sector boundary, renamed the "heliospheric polarity reversal sheet" (HPRS), is truly a two-dimensional surface since open field lines have either one true polarity or the other, whereas the HCS can be distributed through a volume and/or displaced from the HPRS to accommodate the given field configuration. (See also *Kahler et al.* [2003], who illustrate these features in a study of the HCS at solar minimum.)

[13] Field configurations consistent with the observed mismatch intervals are illustrated in Figure 4. In the top left panel, labeled "Type 1," a toward sector follows an away sector, and a loop intervenes. The field points away from the Sun in the leading leg of the loop and toward the Sun in the trailing leg, thus matching the fields in the adjacent sectors. The leading leg of the loop is no longer connected to the Sun, having reconnected with an open field line there. The dashed field line extension from the loop is the outer segment of that open field line and is assumed to lie above or below the plane of Figure 4. Reconnection

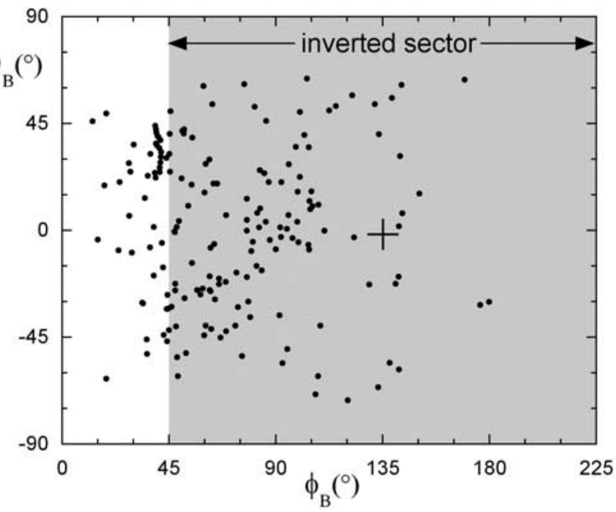

Figure 3. Scatterplot of hourly averages of magnetic azimuth ϕ_B against elevation θ_B in intervals of mismatch between true sector boundaries and local field reversals. Points in the gray area indicate field lines locally inverted from the direction of their true polarity. Inversions tend to be by angles less than the 180°-bend to the opposite Parker spiral direction (cross).

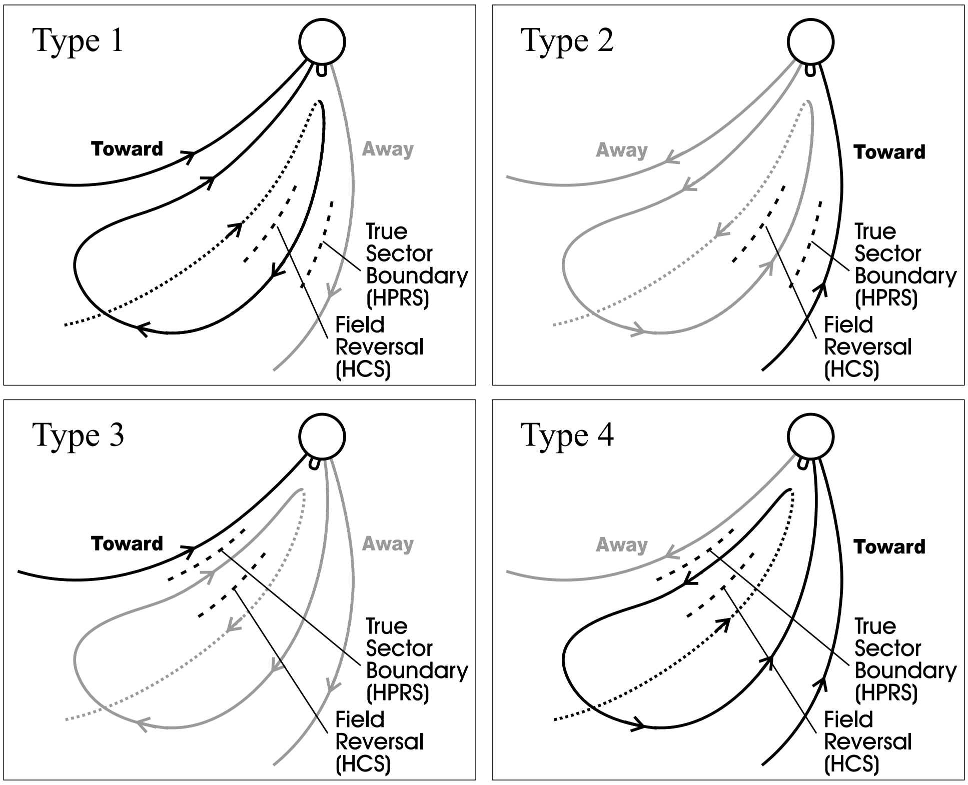

Figure 4. Schematics illustrating how an open loop between fields of opposite polarity can create a separation between the true sector boundary and its associated magnetic field reversal, depending upon the sense of polarity change across the boundary and whether the leading or trailing foot of the loop has been released from the Sun by interchange reconnection.

between an open and closed field line, called "interchange reconnection" by *Crooker et al.* [2002], thus opens closed loops and creates an inverted field line, in this case, in the leading leg of the loop. Although locally pointing away from the Sun in the leading leg, the field comprising the open loop connects back to the Sun with toward polarity. Consequently, the true sector boundary or HPRS lies between the leading leg and the away field line ahead of it, but the field reversal marking the HCS lies between the two legs.

[14] The Type 1 configuration in Figure 4 fits cases in which passage is from the away to the toward sector (A–T) and the HPRS precedes the HCS, leaving locally away-pointing (A) fields in the interval of mismatch, between the dashed lines. The sixth and seventh columns in Table 1 list these two criteria for the first five cases, which are the quasi-recurrent cases in Figure 2, and the last column thus categorizes these cases as Type 1. There are three possible alternatives to Type 1, depending upon the sense of polarity change and whether the leading or trailing leg of the loop is connected to the Sun, and these are illustrated as Types 2–4 in Figure 4. Type 2 is the same as Type 1 except that the sense of polarity change across the sector boundary is reversed (T–A). Since the fields in the legs of the loop match the reversed polarity, the inverted field between the dashed lines now points toward (T) the Sun. Table 1 indicates that the 11 July case fits the Type 2 criteria. Type 3 is the same as Type 1 except that the trailing leg of the loop rather than the leading leg no longer connects to the Sun. The polarity change is the same (A–T), but the trailing leg now comprises the inverted field, which locally points toward (T) the Sun. None of the cases in Table 1 fit the Type 3 criteria. Type 4 is the same as Type 3, except the sense of polarity change is reversed to T–A, which reverses the inverted field to a local direction pointing away (A) from the Sun. Table 1 indicates that the 21 April case fits the Type 4 criteria.

[15] In addition to offering an explanation for the ordering and sense of true sector boundaries and field reversals in intervals of mismatch, Figure 4 also offers an explanation for the systematic tendency for the inverted field to hover near the ortho-Parker-spiral direction, as shown in Figure 3. The discussion of Figure 4 until now has focused on patterns across the legs of the open loop, where the field aligns with the Parker spiral. The assumption has been that the apex of the loop is well beyond the orbit of the observing spacecraft. If, instead, a spacecraft encounters the loop closer to its apex, the field it measures will veer away from the Parker spiral. In the cases of Type 1 and Type 2, Figure 4 shows that the sense of veering will always be toward decreasing ϕ_B because of the systematic way in which the loop field matches the sector structure. For example, in Type 1, $\phi_B = 135°$ in the inverted field line in the leading leg and then gradually shifts toward 45° along the field line outward toward the apex of the loop. In the case of Type 2, ϕ_B shifts from 315° toward 225°. Since all but one of the eight cases plotted in Figure 3 are of Type 1 or Type 2 (where the Type 2 case has been translated to a

virtual inverted away sector), the pattern of decreasing ϕ_B is consistent with the predictions of Figure 4. For Type 3 and Type 4, starting on the trailing leg, the shift is in the opposite direction, toward increasing ϕ_B, but because of the asymmetry introduced by the spiral geometry, the pattern of increasing ϕ_B is more abrupt and possibly more difficult to identify in the data. This may explain why so few Type 3 and Type 4 cases were observed and why the statistical plot of *Kahler et al.* [1998] is heavily weighted toward decreasing ϕ_B. On the other hand, it is possible that Type 1 and Type 2 dominate the data because the leading leg of a loop is greatly favored over the trailing leg for interchange reconnection.

[16] The one exception to the predicted pattern in Figure 4 is the single Type 4 case on 21 April. Although the Type 4 criteria are met, the inversion interval contains values less than the Parker angle of 135°, near 45°, rather than greater than the predicted 135°. These values of ϕ_B, evident in the fifth panel of Figure 2, are not to be found anywhere along the inverted portion of the Type 4 field loop sketched in Figure 4. Apparently, the magnetic configuration in the 21 April case was more complicated than the Type 4 sketch. Another inversion case which meets the Type 4 criteria is one of the two smaller-scale (~5 hour) cases on 17–18 December from Paper 1, mentioned in section 2. The inverted field there, however, lies along the Parker spiral, consistent with passage through the leg of the loop, so it does not provide a test for passage nearer the apex.

[17] The Figure 4 sketches are meant to illustrate only the essence of field inversions at sector boundaries. More complicated configurations undoubtedly occur, as indicated by the spread in magnetic elevation angles in Figure 3. A step up in complication would be to replace the simple open loop in Figure 4 with a coil so that what forms the loop is an open flux rope. This is the configuration used to explain the 8 February case, studied in detail by *Crooker et al.* [1998a], who described it in terms of sector boundary transformation by an open magnetic cloud. More generally, we can now say that field inversions transform sector boundaries. In the wake of the inverted loops in Figure 4 the true sector boundary returns to the location of the HCS field reversal.

[18] The proposed interpretation of field inversions raises two questions. First, if field inversions at sector boundaries are created by an outflow of loops, simple or complicated, what is their relationship to ICMEs? ICMEs and the field inversions analyzed here have many features in common. Their scale sizes are the same, both are observed at sector boundaries (although ICMEs not exclusively so), and their structure reflects formation in the helmet streamer belt [*Crooker et al.*, 1998b; *Kahler et al.*, 1999; *Crooker*, 2000]. In particular, like the loops drawn in Figure 4, *Kahler et al.* [1999] found that the polarity of the magnetic fields in ICME legs is 10 times more likely than not to match the polarity of the surrounding sectors. Table 1 indicates that inversions range from clearly identifiable ICMEs to structures with no ICME signatures at all. Consistent with Table 1, and following *Crooker et al.* [1993], who proposed that transient outflows from the streamer belt cover a range of scale sizes, we suggest that on the large-scale end of that range, they cover a spectrum of form, from quiet outflows of simple loops to recognizable ICMEs, and that inversions lie at the quiet end of that spectrum. One possibility is that inversions are the heliospheric manifestation of the quiet outflows of loops from active regions observed by Yohkoh [*Uchida et al.*, 1992], which would begin under the canopy of the helmet streamer belt.

[19] A difference between inversions and ICMEs is that the magnetic fields in inversions are nearly all open, whereas in ICMEs, on average, signatures of counterstreaming electrons suggest that more than half are closed [*Shodhan et al.*, 2000]. The 8 February case, with its predominantly open magnetic cloud, bridges the two forms, consistent with the idea of a spectrum between them, but the difference between the ends of the spectrum may lie in the nature of the process that drives interchange reconnection. Interchange reconnection is thought to be responsible for the opening of ICMEs [*Crooker et al.*, 2002] as well as field inversions. It is possible that systematic interchange reconnection like that required by the global foot point circulation model of *Fisk et al.* [1999] is part of the release mechanism for loops that comprise inversions (although why it would act on only one leg so as not to disconnect the field lines remains an open question [cf. *Crooker et al.*, 2002]). In contrast, in ICMEs, whatever interchange reconnection has taken place by the time they are observed may have occurred primarily during the brief period of CME liftoff as a consequence of the liftoff process [*Gosling et al.*, 1995]. A search for other interplanetary signatures of interchange reconnection at the Sun, for example, evidence of particle acceleration, might lead to further insights on modes of interchange reconnection.

[20] The second question raised by the proposed interpretation of field inversions is this: If field inversions at sector boundaries are transient structures, how can they also be quasi-recurrent? The same question was raised about ICMEs by *Crooker and Cliver* [1994] and *Crooker and McAllister* [1997] and was addressed as follows. Quasi-recurrence is imposed during the declining phase of the solar cycle by the highly ordered, tilted-dipole geometry at that time. The streamer belt, which serves as a corridor for ICMEs, sweeps past an observing spacecraft at regular intervals. If the CME occurrence rate is still high, the likelihood of encountering one at these regular intervals is also high. In the case of field inversions, the likelihood seems even higher because the release process may be steadier. One can conceive of a limiting scenario in which the process is actually steady state, although this extreme is not borne out in the data.

[21] Finally, to bring to closure the full scope of the work initiated by *Kahler and Lin* [1994, 1995], we consider one more variation of the Figure 4 configurations to illustrate field reversals at localized current sheets away from sector boundaries. These can be achieved by changing the field direction in the loop so that it does not match the surrounding sectors. Figure 5 shows the result applied to Type 1. The true polarity reversal now coincides with its associated field reversal so that the HCS is identical to the HPRS, as is usually assumed, and the field inversion created by interchange reconnection forms two more field reversals. In contrast to Figure 4, however, these reversals are at localized current sheets independent of the HCS. Although one still lies between the legs of the loop, the current there has no topological connection to the HCS, as those in Figure 4 must when considered in three dimensions. The Figure 5

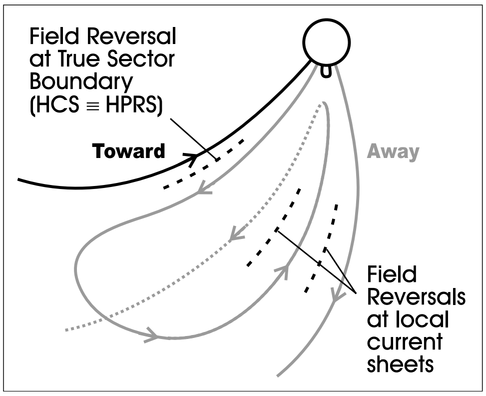

Figure 5. Same as Type 1 in Figure 4 except the polarity of the loop is reversed. The true sector boundary and its associated magnetic field reversal now coincide, and the field inversion creates field reversals at local current sheets independent of the HCS.

configuration thus illustrates the original understanding of field reversals without sector boundaries, which account for most intrasector reversals [*Kahler et al.*, 1996].

4. Conclusions

[22] The findings reported here add to a large body of research supporting the idea that sector boundaries are often the sites of transient outflows and that the largest of these outflows have topological properties intrinsic to the polarity change there. This paper offers a new signature of these transient outflows in the form of large-scale magnetic field inversions at sector boundaries identified by mismatches between polarity reversals in field data and in suprathermal electron pitch angle spectrograms. The signature is consistent with outflows that lie on the quiet end of the spectrum of ICME outflows. The proposed pattern of outflowing loops embedded in the sector structure and magnetically opened by interchange reconnection provides a considerable number of constraints that are met by the data, with only one minor exception. The most important aspect of the proposed pattern is that it offers an explanation for how the HPRS, i.e., the boundary between field lines of truly opposite polarity, independent of any local inversions, can be temporarily separated from the HCS.

[23] **Acknowledgments.** This research was supported by NASA under grants NAG5-10856 and NAG5-10881 and by the National Science Foundation under grant ATM-0119700.

[24] Shadia Rifai Habbal thanks Jack Gosling and another referee for their assistance in evaluating this paper.

References

Crooker, N. U. (2000), Solar and heliospheric geoeffective disturbances, *J. Atmos. Sol. Terr. Phys.*, *62*, 1071–1085.

Crooker, N. U. (2003), Heliospheric current and plasma sheet structure, in *Solar Wind Ten*, edited by M. Velli, R. Bruno, and F. Malara, *AIP Conf. Proc.*, 679, 93–97.

Crooker, N. U., and E. W. Cliver (1994), Postmodern view of M-regions, *J. Geophys. Res.*, *99*, 23,383–23,390.

Crooker, N. U., and A. H. McAllister (1997), Transients associated with recurrent storms, *J. Geophys. Res.*, *102*, 14,041–14,047.

Crooker, N. U., G. L. Siscoe, S. Shodhan, D. F. Webb, J. T. Gosling, and E. J. Smith (1993), Multiple heliospheric current sheets and coronal streamer belt dynamics, *J. Geophys. Res.*, *98*, 9371–9381.

Crooker, N. U., M. E. Burton, G. L. Siscoe, S. W. Kahler, J. T. Gosling, and E. J. Smith (1996a), Solar wind streamer belt structure, *J. Geophys. Res.*, *101*, 24,331–24,341. (Correction, *J. Geophys. Res.*, *102*, 4741, 1997.)

Crooker, N. U., A. J. Lazarus, R. P. Lepping, K. W. Ogilvie, J. T. Steinberg, A. Szabo, and T. G. Onsager (1996b), A two-stream, four-sector, recurrence pattern: Implications from WIND for the 22-year geomagnetic activity cycle, *Geophys. Res. Lett.*, *23*, 1275–1278.

Crooker, N. U., et al. (1998a), Sector boundary transformation by an open magnetic cloud, *J. Geophys. Res.*, *103*, 26,859–26,868.

Crooker, N. U., J. T. Gosling, and S. W. Kahler (1998b), Magnetic clouds at sector boundaries, *J. Geophys. Res.*, *103*, 301–306.

Crooker, N. U., J. T. Gosling, and S. W. Kahler (2002), Reducing heliospheric magnetic flux from coronal mass ejections without disconnection, *J. Geophys. Res.*, *107*(A2), 1028, doi:10.1029/2001JA000236.

Crooker, N. U., D. E. Larson, S. W. Kahler, S. M. Lamassa, and H. E. Spence (2003), Suprathermal electron isotropy in high-beta solar wind and its role in heat flux dropouts, *Geophys. Res. Lett.*, *30*(12), 1619, doi:10.1029/2003GL017036.

Crooker, N. U., C.-L. Huang, S. M. Lamassa, D. E. Larson, S. W. Kahler, and H. E. Spence (2004), Heliospheric plasma sheets, *J. Geophys. Res.*, *109*, A03107, doi:10.1029/2003JA010170.

Fisk, L. A., T. H. Zurbuchen, and N. A. Schwadron (1999), On the coronal magnetic field: Consequences of large-scale motion, *Astrophys. J.*, *521*, 868–877.

Gosling, J. T., J. Birn, and M. Hesse (1995), Three-dimensional magnetic reconnection and the magnetic topology of coronal mass ejection events, *Geophys. Res. Lett.*, *22*, 869–872.

Kahler, S., and R. P. Lin (1994), The determination of interplanetary magnetic field polarities around sector boundaries using $E > 2$ keV electrons, *Geophys. Res. Lett.*, *21*, 1575–1578.

Kahler, S., and R. P. Lin (1995), An examination of directional discontinuities and magnetic polarity changes around interplanetary sector boundaries using $E > 2$ keV electrons, *Sol. Phys.*, *161*, 183–195.

Kahler, S. W., N. U. Crooker, and J. T. Gosling (1996), The topology of intrasector reversals of the interplanetary magnetic field, *J. Geophys. Res.*, *101*, 24,373–24,382.

Kahler, S. W., N. U. Crooker, and J. T. Gosling (1998), Properties of interplanetary magnetic sector boundaries based on electron heat-flux flow directions, *J. Geophys. Res.*, *103*, 20,603–20,612.

Kahler, S. W., N. U. Crooker, and J. T. Gosling (1999), The polarities and locations of interplanetary coronal mass ejections in large interplanetary magnetic sectors, *J. Geophys. Res.*, *104*, 9919–9924.

Kahler, S. W., N. U. Crooker, and D. E. Larson (2003), Probing the magnetic polarity structure of the heliospheric current sheet, *J. Geophys. Res.*, *108*(A8), 1316, doi:10.1029/2002JA009649.

Lepping, R. L., et al. (1995), The Wind magnetic field investigation, *Space Sci. Rev.*, *71*, 207–229.

Lin, R. P., et al. (1995), A three-dimensional plasma and energetic particle investigation for the Wind spacecraft, *Space Sci. Rev.*, *71*, 125–153.

Ogilvie, K. W., et al. (1995), SWE: A comprehensive plasma instrument for the Wind spacecraft, *Space Sci. Rev.*, *71*, 55–77.

Richardson, I. G., and H. V. Cane (1995), Regions of abnormally low proton temperature in the solar wind (1965–1991) and their association with ejecta, *J. Geophys. Res.*, *100*, 23,397–23,412.

Shodhan, S., N. U. Crooker, S. W. Kahler, R. J. Fitzenreiter, D. E. Larson, R. P. Lepping, G. L. Siscoe, and J. T. Gosling (2000), Counterstreaming electrons in magnetic clouds, *J. Geophys. Res.*, *105*, 27,261–27,268.

Szabo, A., D. E. Larson, and R. P. Lepping (1999), The heliospheric current sheet on small scale, in *Solar Wind Nine*, edited by S. Habbal et al., *AIP Conf. Proc.*, 471, 589–592.

Uchida, Y., A. McAllister, K. T. Strong, Y. Ogawara, T. Shimuzu, R. Matsumoto, and H. S. Hudson (1992), Continual expansion of the active-region corona observed by the Yohkoh soft X-ray telescope, *Publ. Astron. Soc. Jpn.*, *44*, L155–L160.

N. U. Crooker, Center for Space Physics, Boston University, 725 Commonwealth Avenue, Boston, MA 02215, USA. (crooker@bu.edu)

S. W. Kahler, Air Force Research Laboratory, 29 Randolph Road, Hanscom AFB, MA 01731-3010, USA. (stephen.kahler@hanscom.af.mil)

D. E. Larson and R. P. Lin, Space Sciences Laboratory, University of California, Berkeley, Centennial at Grizzly Peak, Berkeley, CA 94720, USA. (davin@ssl.berkeley.edu; rlin@ssl.berkeley.edu)